Targeted mutation of the murine arylhydrocarbon receptor nuclear translocator 2 (*Arnt2*) gene reveals partial redundancy with *Arnt*

Brian Keith*†, David M. Adelman‡, and M. Celeste Simon†§¶‖

Departments of *Medicine and §Cell and Developmental Biology, †Abramson Family Cancer Research Institute, and ¶Howard Hughes Medical Institute, University of Pennsylvania, 421 Curie Boulevard, Philadelphia, PA 19104; and ‡Department of Pathology, University of Chicago, 5841 South Maryland Avenue, Chicago, IL 60637

Edited by Steven L. McKnight, University of Texas Southwestern Medical Center, Dallas, TX, and approved April 11, 2001 (received for review October 18, 2000)

The ubiquitously expressed basic helix–loop–helix (bHLH)-PAS protein ARNT (arylhydrocarbon receptor nuclear transporter) forms transcriptionally active heterodimers with a variety of other bHLH-PAS proteins, including HIF-1α (hypoxia-inducible factor-1α) and AHR (arylhydrocarbon receptor). These complexes regulate gene expression in response to hypoxia and xenobiotics, respectively, and mutation of the murine *Arnt* locus results in embryonic death by day 10.5 associated with placental, vascular, and hematopoietic defects. The closely related protein ARNT2 is highly expressed in the central nervous system and kidney and also forms complexes with HIF-1α and AHR. To assess unique roles for ARNT2 in development, and reveal potential functional overlap with ARNT, we generated a targeted null mutation of the murine *Arnt2* locus. *Arnt2*$^{-/-}$ embryos die perinatally and exhibit impaired hypothalamic development, phenotypes previously observed for a targeted mutation in the murine bHLH-PAS gene *Sim1* (Single-minded 1), and consistent with the recent proposal that ARNT2 and SIM1 form an essential heterodimer *in vivo* [Michaud, J. L., DeRossi, C., May, N. R., Holdener, B. C. & Fan, C. (2000) *Mech. Dev.* 90, 253–261]. In addition, cultured *Arnt2*$^{-/-}$ neurons display decreased hypoxic induction of HIF-1 target genes, demonstrating formally that ARNT2/HIF-1α complexes regulate oxygen-responsive genes. Finally, a strong genetic interaction between *Arnt* and *Arnt2* mutations was observed, indicating that either gene can fulfill essential functions in a dose-dependent manner before embryonic day 8.5. These results demonstrate that *Arnt* and *Arnt2* have both unique and overlapping essential functions in embryonic development.

Transcriptional responses to many environmental and developmental stimuli are mediated by the basic helix–loop–helix (bHLH)-PAS family of proteins, which form heterodimers that bind regulatory DNA sequences in promoter and enhancer elements (1). The bHLH-PAS protein ARNT (arylhydrocarbon nuclear receptor translocator) regulates the expression of different sets of genes in response to distinct environmental challenges. For example, ARNT forms a complex with the arylhydrocarbon receptor (AHR) to activate expression of genes encoding cytochromes P450 and other proteins involved in metabolism of xenobiotic compounds (2, 3). In addition, ARNT dimerizes with hypoxia-inducible factor (HIF)-1α, or the closely related proteins HIF-2α or HIF-3α, in response to low oxygen concentrations (hypoxia) to induce the expression of hypoxia-regulated genes encoding vascular endothelial growth factor (VEGF), glucose transporters, and many glycolytic enzymes (4, 5). Recent reports have suggested that the relative activity of these different transcriptional programs may be determined by competition between AHR and HIF-1α proteins for binding to ARNT (6).

Targeted mutation of the murine *Arnt* locus results in embryonic lethality between embryonic day 9.5 (E9.5) and E10.5, characterized by disrupted placental, hematopoietic, and yolk sac vascular development (7–9). Interestingly, the vascular and developmental phenotypes of *Hif-1α* mutant embryos are comparatively more severe at E9.5 than those observed in *Arnt* mutant mice (10, 11), suggesting that other proteins can partly compensate for the loss of ARNT in regulating hypoxia-regulated genes essential for early embryogenesis. We and others have shown that ARNT2, an ARNT homolog highly expressed in brain and kidney, can form functional complexes with HIF-1α (12) and AHR (13), implying that ARNT2 and ARNT may have partly overlapping functions *in vivo*. To investigate this possibility, and to determine any unique developmental roles attributable to ARNT2, we generated a targeted mutation of the murine *Arnt2* locus.

In contrast to *Arnt* mutants, *Arnt2*$^{-/-}$ embryos appear to develop normally but die perinatally. Interestingly, perinatal lethality has also been reported for mice with a targeted mutation of another bHLH-PAS gene, *Sim1* (14), and is associated with loss of neuroendocrine lineages that regulate pituitary function by secreting oxytocin (OT), arginine-vasopressin (AVP), thyrotropin-releasing hormone (TRH), corticotropin-releasing hormone (CRH), and somatostatin (SS). Expression of genes encoding these five hormones is down-regulated in *Sim1*$^{-/-}$ embryos and is correlated with the death, or change in fate, of the corresponding neurons (14). The perinatal lethality of both *Sim1*$^{-/-}$ and *Arnt2*$^{-/-}$ embryos raised the possibility that SIM1 and ARNT2 proteins may interact *in vivo*. While we were conducting our experiments, a report was published showing similar hypothalamic defects in a different mouse strain (c^{112k}) that harbors a deletion of chromosome 7 including the *Arnt2* coding sequences (15). Analysis of c^{112k} embryos showed down-regulation of the same neuroendocrine target genes observed in *Sim1*$^{-/-}$ embryos, consistent with the proposal that ARNT2 and SIM1 form a functional heterodimer *in vivo* (16). Although the hypothalamic phenotypes cosegregated with loss of the *Arnt2* gene in the c^{112k} background, the extent of possible genetic interactions between *Arnt2* and other loci deleted in this strain could not be ascertained. We show here that targeted disruption of the murine *Arnt2* locus results in neuroendocrine phenotypes similar to those reported for the c^{112k} strain. In addition, the *Arnt2*$^{-/-}$ mutation confers subtle hypoxic phenotypes and displays a strong genetic interaction with a mutant *Arnt* allele,

This paper was submitted directly (Track II) to the PNAS office.

Abbreviations: bHLH, basic helix–loop–helix; ARNT, arylhydrocarbon nuclear receptor translocator; HIF, hypoxia-inducible factor; Sim, Single-minded; VEGF, vascular endothelial growth factor; E*n*, embryonic day *n*; EMSA, electrophoretic mobility-shift assay; PVN, paraventricular nucleus; SON, supraoptic nucleus; CNS, central nervous system.

‖To whom reprint requests should be addressed at: Howard Hughes Medical Institute, Abramson Cancer Research Institute, University of Pennsylvania School of Medicine, BRB II/III Room 456, 421 Curie Boulevard, Philadelphia, PA 19104. E-mail: celeste2@mail.med.upenn.edu.

The publication costs of this article were defrayed in part by page charge payment. This article must therefore be hereby marked "*advertisement*" in accordance with 18 U.S.C. §1734 solely to indicate this fact.

 www.pnas.org/cgi/doi/10.1073/pnas.121494298

indicating that *Arnt2* and *Arnt* have both unique and overlapping functions in development.

Materials and Methods

Generation of *Arnt2* Mutant Allele. λ phage clones that hybridized to an *Arnt2* bHLH-domain cDNA probe were purified from a 129 SVJ mouse genomic library (Stratagene). A 1.2-kbp *Sac*I–*Kpn*I fragment immediately 3′ to the bHLH-encoding exon was amplified (forward primer, 5′-GCACTGCAGGTGGGAACCATGTCGGAG; reverse primer, 5′-CCGAATCAGACACGTAGATGACTCTCC) and subcloned into Bluescript II (Stratagene). This insert was cloned as an *Eco*RI/*Kpn*I fragment into a modified pPNT vector (17). A 7-kbp fragment immediately 5′ to the bHLH-encoding exon, but retaining the splice acceptor site and the first 91 nucleotides of bHLH coding sequence, was amplified (forward primer, 5′-GCGATCGATATTATGTCATCGCCCTTTGAACTT; reverse primer, 5′-ACTGCGGCCGCTGTGGTTCTCTCTTCCCAGAAAGCAAG) and cloned into the pPNT vector containing the 1.2-kbp 3′ fragment. This targeting vector was electroporated into RW murine embryonic stem cells (Incyte Genomics, Palo Alto, CA) as previously described (7). G418-resistant, ganciclovir-resistant embryonic stem cell clones were genotyped by PCR analysis (94°C for 1 min, 58°C for 1 min, 72°C for 2 min for 30 cycles) with primers specific for the wild-type allele (forward primer, 5′-TGCACTGGCTAGGAAGCCAGACAA), the mutant allele (forward primer, 5′-GCCTGCTCTTTACTGAAGGCTCTTG), and a shared reverse primer (5′-ATGCTCTGCACCGCACAGCTAATG). Southern blot analysis was performed with probes derived from fragments located immediately 5′ and 3′ to the sequences used to make the targeting vector. Heterozygous cells were injected into E3.5 blastocysts and transferred into pseudopregnant mice as previously described (7). Highly chimeric (90%) male mice were mated to C57BL6 females, and germ-line transmission of one clone (no. 536) was confirmed by PCR and Southern blot analysis (Fig. 1*B*).

RNA *in Situ* Hybridization. E9.5, E13.5, and E18.5 embryos from $Arnt2^{+/-}$ matings were fixed in 4% paraformaldehyde for 48 h. Genotypic analysis was performed by PCR on yolk sac DNA. Subsequent tissue embedding, sectioning, and *in situ* hybridization were performed as previously described (18). *Brn2* and *Trh* RNA probes were generated from reverse transcription–PCR-amplified gene-specific fragments (*Brn2*, forward primer 5′-AAGCAATTCAAGCAGAGGCG; reverse primer 5′-CTACTTCATTGCCTGGGTAC) (*Trh*, forward primer 5′-CTGCCAACCAAGACAAGGAT; reverse primer 5′-CAATCCTACCCTTTCTGAGG). Sense and antisense RNA probes were generated by using T7 and Sp6 RNA polymerases and α-[^{35}S]thio-UTP as described (18). Vasopressin RNA was detected by using an antisense oligodeoxynucleotide (5′-GTATACCCGGGGCTTGGCAGAATCCACGGACTCTTGTGTCCCAGCCAG) that was 3′ end-labeled by using terminal deoxynucleotidyltransferase and α-[^{35}S]thio-dATP as described (19). *Pgk*, *Glut3*, and *Vegf* probes were generated by reverse transcription–PCR with the following primers: *Pgk,* 5′ 5′-CTTGGACTGTGGTACTGAGAG and 3′ 5′-CTGAATCTTGCGCTAACACCA; *Glut3,* 5′ 5′-GCCTTCTTTGAGATTGGACC and 3′ 5′-CATTGGCGATCTGGTCAACC; and *Vegf,* 5′ 5′-CCATGCAGATCATGCGGATC and 3′ 5′-CAAAGTTCTCCTCGAAGGATC. Hybridization to sense probes revealed only low levels of general background staining (data not shown).

Cortical Neuron Cultures. Cerebral hemispheres from E14.5 embryos were dissected and cortical neurons were cultured as previously described (12). After 7 days of culture under an atmosphere of 21% O_2/5% CO_2/74% N_2, samples were transferred to an incubator (Jouan, Winchester, VA) maintained at 3% O_2/5% CO_2/92% N_2 for hypoxic induction. Nuclear extracts were prepared as described (12) after 4 h of hypoxic induction, and RNA was prepared by Trizol extraction (GIBCO/Life Technologies) after 16 h of induction.

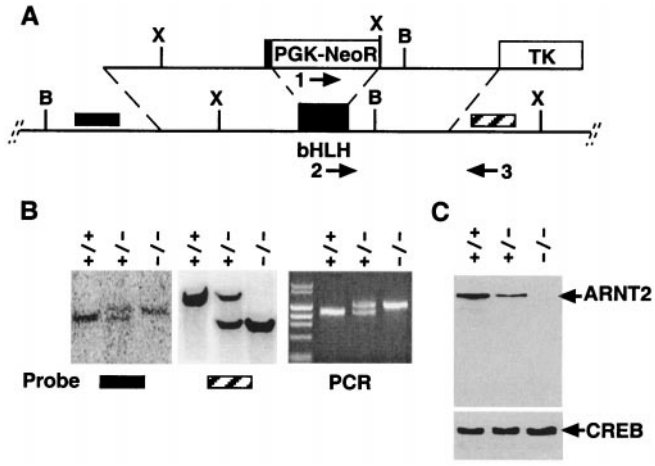

Fig. 1. Targeted disruption of murine *Arnt2* gene. (*A*) Schematic diagram of targeting vector (upper line) and *Arnt2* genomic locus (lower line) including the bHLH domain-encoding exon (*PGK-Neo*^{R}, phosphoglycerate kinase–neomycin phosphotransferase gene cassette; *TK*, PGK-thymidine kinase gene cassette). X, *Xba*I sites; B, *Bam*HI sites. Arrows 1–3 refer to PCR primers for distinguishing mutant (1 and 3) from wild-type (2 and 3) loci. Hatched box refers to 3′, and solid box to 5′ Southern blot probes. (*B*) Southern blot and PCR analyses of $Arnt2^{+/+}$, $Arnt2^{+/-}$, and $Arnt2^{-/-}$ embryos. (*Left*) Hybridization of the 5′ probe (solid bar) to *Bam*HI-digested DNA, reflecting insertion of the *PGK-Neo*^{R} cassette (wild-type locus, 7 kbp, mutant locus; 8.2 kbp). (*Center*) Introduction of new *Xba*I site by using 3′ probe (hatched bar) (wild-type locus, 9 kbp; mutant locus, 5 kbp). (*Right*) PCR analysis of $Arnt2^{+/+}$, $Arnt2^{+/-}$, and $Arnt2^{-/-}$ embryo DNA, where the lower (1200-bp) band corresponds to the wild-type locus and the larger (1400-bp) band, to the mutant locus. (*C*) Western blot analysis of nuclear extracts from cultured E14.5 cortical neurons with ARNT2 antibodies. The same filter was stripped and reprobed with CREB antibodies to control for loading.

Molecular and Immunohistochemical Techniques. Northern blot and electrophoretic mobility-shift assay (EMSA) analyses were conducted, and ARNT2 antibodies were prepared, as previously described (12). Polyclonal ARNT antibodies were obtained from Novus Biologicals (Littleton, CO) and CREB (cAMP response element binding protein) antibodies were from New England Biolabs. PECAM (CD31) immunohistochemistry was performed as described (20) with MEC13.3 antibodies (Santa Cruz Biotechnology). DNA was extracted from mouse tail clips, or from dissected E8.5 yolk sacs as described (7).

Results

Generation of the *Arnt2* Null Mutant Allele. Genomic DNA fragments surrounding the bHLH-encoding exon of the murine *Arnt2* gene were amplified and inserted into the pPNT vector (17) to generate the targeting construct shown in Fig. 1*A*. Homologous recombination of this construct with the wild-type *Arnt2* locus replaced most of the *Arnt2* bHLH exon with the *Pgk-Neo* gene cassette. Two homologous recombinant embryonic stem cell lines were obtained from 860 neomycin-resistant, ganciclovir-resistant clones, as determined by Southern blot and PCR analyses (Fig. 1*B*). One colony (no. 536) produced fertile chimeric male mice that transmitted the recombinant allele. $Arnt2^{+/-}$ mice were fertile and showed no obvious morphological or developmental phenotypes. However, the lack of live-born $Arnt2^{-/-}$ pups (Table 1) indicated that the mutant allele was

Table 1. Segregation of *Arnt2* mutant allele

Mice	Number found		
	$Arnt2^{+/+}$	$Arnt2^{+/-}$	$Arnt2^{-/-}$
Liveborn pups	28	59	0
E18.5 embryos	11	26	14

lethal when homozygous. Dissection of late stage (E18.5) embryos revealed that $Arnt2^{-/-}$ progeny were represented in expected Mendelian ratios (Table 1), suggesting that homozygous mutant mice were dying perinatally. E18.5 $Arnt2^{-/-}$ embryos displayed no obvious morphological defects in the kidney, and the cleft palate and thymic defects reported for c^{112k} homozygous mutants (15) were not observed (data not shown). Rare (≈2% of expected) $Arnt2^{-/-}$ pups survived birth, although these animals remained severely runted and died after 7–10 days.

RNA *in situ* hybridization and Northern blot analysis of $Arnt2^{-/-}$ embryos indicated that the *Arnt2* locus is still transcribed in homozygous mutant animals (data not shown). However, Western blot analysis of neuronal protein extracts showed decreased ARNT2 protein in heterozygous mutant neurons, and a complete absence of ARNT2 protein in homozygous mutants (Fig. 1*C*). Together, these results indicate that we have generated a null *Arnt2* mutant allele.

***Arnt2* Mutation Associated with Loss of Neuroendocrine Cell-Specific Gene Expression.** Establishment of the hypothalamic–pituitary axis requires the function of magnocellular and parvocellular neurons in the hypothalamic paraventricular nucleus (PVN) and supraoptic nucleus (SON). Briefly, magnocellular neurons project from the PVN and SON directly to the posterior pituitary, where they secrete oxytocin (OT) and arginine-vasopressin (AVP). In contrast, parvocellular neurons in the PVN and anterior periventricular nucleus secrete thyrotropin-releasing hormone (TRH), corticotropin-releasing hormone (CRH), and somatostatin (SS) into the portal vasculature connecting the median eminence to the anterior pituitary. In $Sim1^{-/-}$ embryos, these lineages fail to differentiate or survive, as indicated by decreased expression of neuropeptide-encoding genes (14). Furthermore, the expression of transcripts encoding BRN2, a POU-domain transcription factor essential for the development of AVP, OT, and CRH-producing neurons (21), is down-regulated in $Sim1^{-/-}$ embryos, placing *Brn2* expression downstream of *Sim1* (14). Identical phenotypes were reported for *Arnt2*-deficient c^{112k} mutants, leading Michaud *et al.* (16) to propose that ARNT2 and SIM1 form functional heterodimers *in vivo*.

To confirm that loss of *Arnt2* function is sufficient to disrupt hypothalamic development, we analyzed the expression of neuropeptide genes in wild-type and $Arnt2^{-/-}$ mice by RNA *in situ* hybridization (Fig. 2). Transcripts marking representative parvocellular and magnocellular neurons (*Trh* and *Avp*, respectively) were down-regulated in the PVN and SON of $Arnt2^{-/-}$ embryos (Fig. 2). Importantly, the expression of *Brn2* was also down-regulated in the PVN and SON of $Arnt2^{-/-}$ mice. These results confirm that loss of ARNT2 accounts for the hypothalamic phenotype observed in the c^{112k} strain, and does not result from genetic interactions with other deleted loci.

ARNT2 in Neural Responses to Hypoxia. We have shown recently that ARNT2 forms functional DNA-binding heterodimeric complexes with HIF-1α in transfected hepatocytes. Moreover, ARNT2/HIF-1α complexes are detected in primary mixed cortical cultures, hippocampal cultures, and NGF-induced PC12 cells (12). Interestingly, ARNT2/HIF-1α heterodimers constitute approximately one-half of the DNA-binding HIF complexes detected in these cells, whereas ARNT/HIF-1α accounts for the remainder (12). To assess the effects of *Arnt2* mutation on hypoxia-regulated gene expression, we pooled cortical neuron cultures from two independent E14.5 wild-type or two independent E14.5 $Arnt2^{-/-}$ embryos. Northern blot analyses indicated that several oxygen-responsive genes (*Pgk, Vegf, Glut3*) are induced by 16 h of hypoxia in both wild-type and homozygous *Arnt2* mutant neurons (Fig. 3*A*). However, quantitation of

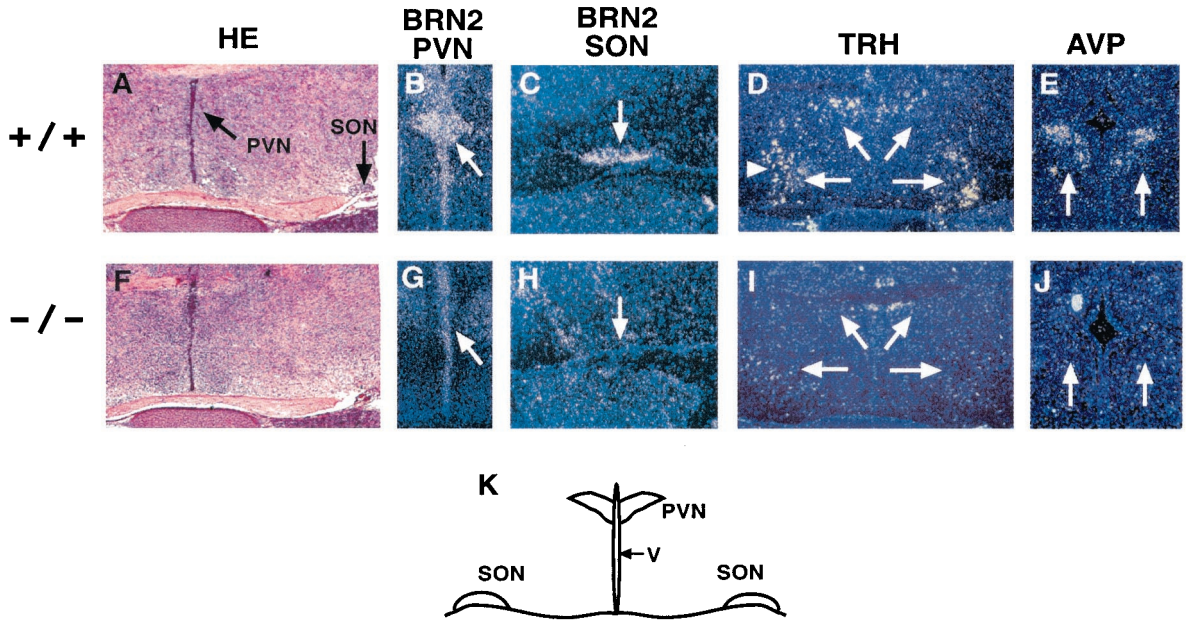

Fig. 2. RNA *in situ* hybridization analysis of PVN and SON of $Arnt2^{+/+}$ and $Arnt2^{-/-}$ E18.5 embryos.(*A* and *F*) Hematoxylin and eosin staining of $Arnt2^{+/+}$ coronal hypothalamic sections. Arrows indicate PVN and SON. Hybridization patterns of *Brn2* (*B, C, G,* and *H*), *Trh* (*D* and *I*), and *Avp* (*E* and *J*) transcripts in $Arnt2^{+/+}$ (upper row) and $Arnt2^{-/-}$ (lower row) embryos are shown. For each probe, note decreased signal intensity in $Arnt2^{-/-}$ embryos relative to $Arnt2^{+/+}$ embryos (arrows). (*K*) Schematic diagram of coronal section, outlining the third ventricle (V), PVN, and SON. (*A* and *F,* ×50; *B–E* and *G–J,* ×100.)

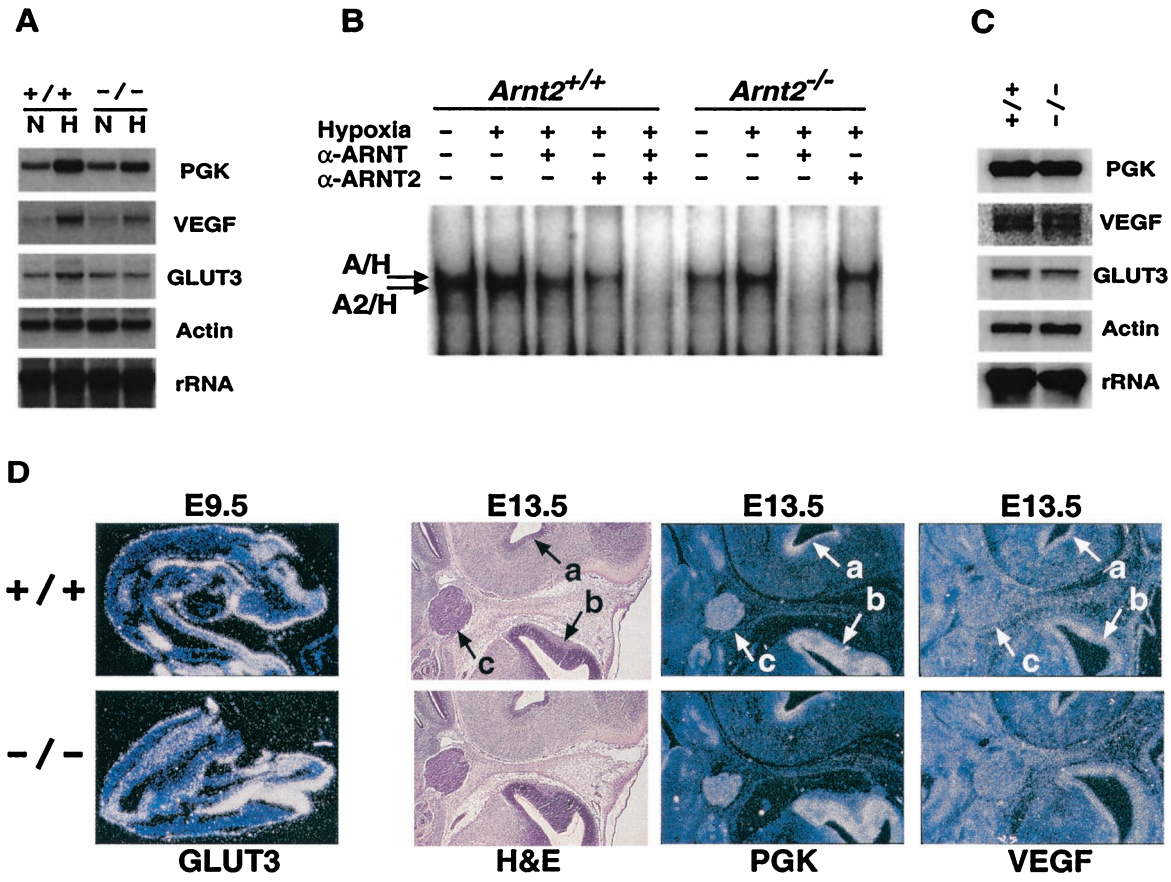

Fig. 3. RNA, EMSA, and *in situ* hybridization analysis of *Arnt2*$^{+/+}$ and *Arnt2*$^{-/-}$ neurons and embryos. (*A*) Northern blot analysis of RNA from E14.5 cortical neuron cultures maintained at 21% O_2 (N) or subjected to 3% O_2 for 16 h (H). A single blot was hybridized sequentially to probes for murine phosphoglycerate kinase (*Pgk*), VEGF (*Vegf*), glucose transporter 3 (*Glut3*), α-actin, or 18S rRNA. (*B*) EMSA analysis showing HIF DNA-binding complexes in cultured cortical neurons. ARNT/HIF-1α complexes migrate slightly slower than ARNT2/HIF-1α complexes in this assay (12). Antibodies specific for ARNT (α-ARNT) and ARNT2 (α-ARNT2) were included to ablate each complex independently. *Arnt2*$^{+/+}$ neurons contain a mixture of ARNT/HIF-1α (denoted A/H) and ARNT2/HIF-1α (denoted A2/H) complexes, whereas *Arnt2*$^{-/-}$ neurons contain only ARNT/HIF-1α complexes. HIF complex levels in nuclear extracts from normoxic primary cultures vary between experiments (12). (C) Northern blot analysis of RNA from cortical neurons maintained at 5% O_2 for 7 days. A single blot was hybridized sequentially to the same probes used in *A*. (*D*) Representative RNA *in situ* hybridization analyses of HIF-1 target genes in *Arnt2*$^{+/+}$ and *Arnt2*$^{-/-}$ E9.5 embryos (*Glut3*, ×100) and E13.5 central nervous system (CNS) (*Pgk* and *Vegf*, ×50), respectively. Equivalent patterns and levels of RNA expression were also observed in both genotypes for *Pgk* and *Vegf* in E9.5 embryos and *Glut3* in E13.5 CNS (data not shown). H&E, hematoxylin and eosin staining. a, Third ventricle; b, lateral ventricle; c, trigeminal ganglion.

radioactive signals (normalized to 18S RNA) revealed that the hypoxic induction of *Pgk*, *Vegf*, and *Glut3* RNA is reduced by 24% ± 3% in *Arnt2*$^{-/-}$ neurons relative to *Arnt2*$^{+/+}$ neurons. EMSA analysis of cortical neuron nuclear extracts made from parallel cultures detected both ARNT/HIF-1α and ARNT2/HIF-1α complexes in wild-type neurons (Fig. 3*B*), as previously shown (12). In contrast, only ARNT/HIF-1α complexes were detected in the *Arnt2*$^{-/-}$ mutant neurons, providing a mechanism whereby hypoxia-responsive genes can still be induced in these cells (Fig. 3*B*).

It is possible that the kinetics of hypoxic gene induction are slower in *Arnt2*$^{-/-}$ neurons cultured *in vitro* because of the lack of ARNT2/HIF-1α, but that residual ARNT/HIF-1α complexes are sufficient to maintain normal steady-state levels of target gene expression in the *Arnt2*$^{-/-}$ CNS *in vivo*. To address this possibility, we maintained neuronal cultures for a prolonged period (7 days) at a physiologically relevant O_2 concentration (5% O_2) (4). Fig. 3*C* shows equivalent expression levels of *Pgk*, *Vegf*, and *Glut3* transcripts in both wild-type and *Arnt2*$^{-/-}$ neurons, consistent with this hypothesis. RNA *in situ* hybridization analyses of E9.5 embryos and E13.5 CNS (Fig. 3*D*) also displayed highly similar levels and patterns of HIF-1 target gene expression in *Arnt2*$^{+/+}$ and *Arnt2*$^{-/-}$ embryos (very subtle differences in *Vegf* expression in localized regions of the *Arnt2*$^{+/+}$ and *Arnt2*$^{-/-}$ E13.5 brain may be evident). This model is also consistent with the observation that CNS vascularization in the cranial region of E9.5 *Arnt2*$^{-/-}$ mutant embryos was indistinguishable from wild type as revealed by PECAM immunohistochemistry (Fig. 4 *A* and *B*). In contrast, *Arnt*$^{-/-}$ embryos show dramatic alterations in cranial vascularity at this stage (Fig. 4 *C* and *D*), suggesting that ARNT plays a predominant role in regulating VEGF expression *in vivo*. Taken together with our previous demonstration of ARNT2/HIF-1α-mediated hypoxic gene expression (12), these data indicate that ARNT2/HIF-1α complexes can regulate known HIF-1 target genes, but that ARNT/HIF-1α complexes retained in *Arnt2*$^{-/-}$ cells are sufficient to regulate normal hypoxic responses *in vivo*.

Dose-Dependent Requirement for *Arnt* or *Arnt2* Before E8.5. To reveal possible genetic interactions between *Arnt* and *Arnt2*, we crossed compound heterozygous mutant *Arnt*$^{+/-}$, *Arnt2*$^{+/-}$ mice. As *Arnt*$^{-/-}$ mice die between E9.5 and E10.5, we dissected E8.5 embryos and prepared DNA from each (n = 67). Genotypes were determined by PCR analysis, and were distributed as shown

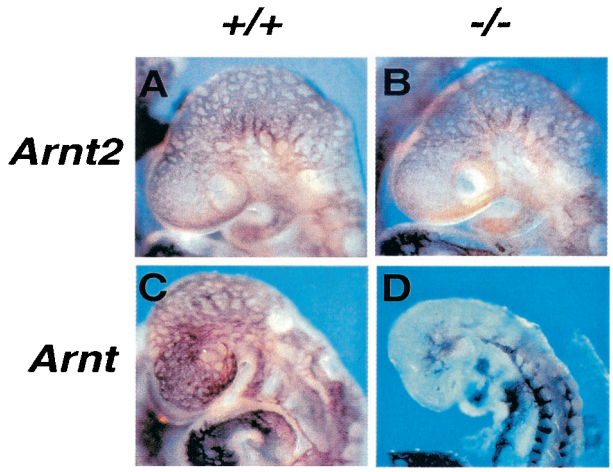

Fig. 4. PECAM immunohistochemistry on E9.5 embryos. (*A* and *B*) Embryos segregating the *Arnt2* mutation. (*C* and *D*) Embryos segregating the *Arnt* mutation. Note disrupted cranial vascular development in *D*. (×140.)

in the upper half of Table 2. As *Arnt* and *Arnt2* are unlinked, homozygous double mutants would be expected to constitute 1/16 of the total. Interestingly, only 1 $Arnt^{-/-}$, $Arnt2^{+/-}$ embryo and 1 $Arnt^{+/-}$, $Arnt2^{-/-}$ embryo were recovered (as compared with 8.4 expected for each genotype), and no homozygous double mutants were observed (4.2 expected). These data are inconsistent with expected Mendelian distributions ($P = 0.005$) and suggest that the vast majority of embryos lacking at least two wild-type alleles of either *Arnt* or *Arnt2* are resorbed before E8.5. If a genetic model is invoked that assumes the early lethality of these embryos, then the number of expected genotypes is reduced from 9 to 6, and the predicted distribution of genotypes closely matches the observed distribution ($P = 0.85$, lower half of Table 2). These data are consistent with a model in which either *Arnt* or *Arnt2* can fulfill one or more overlapping essential functions in a dose-dependent fashion before E8.5.

Table 2. $Arnt^{+/-}$, $Arnt2^{+/-}$ × $Arnt^{+/-}$, $Arnt2^{+/-}$ matings

Arnt	*Arnt2*	No. expected	No. observed
Assuming Mendelian inheritance of all genotypes			
+/+	+/+	4.2	6
+/+	−/−	4.2	5
−/−	+/+	4.2	4
−/−	−/−	4.2	**0**
+/+	+/−	8.4	10
+/−	+/+	8.4	15
+/−	+/−	16.8	25
+/−	−/−	8.4	**1**
−/−	+/−	8.4	**1**
$n = 67$; $P = 0.005$			
Modified genetic model			
+/+	+/+	6.1	6
+/+	−/−	6.1	5
−/−	+/+	6.1	4
+/+	+/−	12.2	10
+/−	+/+	12.2	15
+/−	+/−	24.4	25
+/−	−/−	0	1
−/−	+/−	0	1
−/−	−/−	0	0
$n = 67$; $P = 0.85$*			

*Calculated for first six genotypes listed.

Discussion

The bHLH-PAS protein ARNT regulates the expression of many different genes in response to distinct environmental and developmental signals (1, 22). ARNT and ARNT2 share a high degree of sequence similarity (13), raising the possibility that they may have at least partly redundant functions in development. Previous analysis, however, demonstrated that the two genes are expressed in nonidentical patterns in the developing mouse embryo. Whereas both genes are expressed at detectable levels in most organ systems at E9.5 and E13.5, *Arnt* transcripts appear to be expressed at highest levels in organs outside the CNS, whereas the highest levels of *Arnt2* RNA expression are observed in the developing CNS and kidney (18). These data, as well as the relatively early arrest of $Arnt^{-/-}$ embryos (E9.5–E10.5) (7, 8), argue strongly that normal ARNT2 expression cannot fully compensate for the loss of ARNT. Whether these unique functions are a result of different expression patterns or inherent biochemical differences between the proteins is not yet clear.

To investigate the developmental functions of ARNT2, we created a targeted mutation of the murine *Arnt2* locus. The aberrant hypothalamic development and perinatal lethality we observed in $Arnt2^{-/-}$ embryos are very similar to the findings in the previously described *Arnt2*-deficient c^{112k} deletion strain (16), confirming that these phenotypes can be attributed to the loss of *Arnt2* alone, and apparently do not require the loss of other loci deleted in the c^{112k} strain. Moreover, our data are consistent with the model proposed by Michaud *et al.* (16) that ARNT2/SIM1 heterodimers are required for neuron survival or terminal differentiation in the developing PVN and SON. This model is supported by the observation that *Brn2* expression in the PVN and SON is not maintained in the absence of either ARNT2 or SIM1.

We also observed subtle changes in the level of hypoxic target gene induction in $Arnt2^{-/-}$ cortical neurons cultured *in vitro*. After 16 h of hypoxic treatment, *Pgk*, *Vegf,* and *Glut3* transcript levels were induced in $Arnt2^{-/-}$ neurons to only 75% of the wild-type controls, suggesting that ARNT2/HIF-1α complexes can regulate these known HIF-1 target genes. However, the presence of residual ARNT/HIF-1α complexes is apparently sufficient to maintain steady-state target gene expression *in vivo* under conditions of physiological hypoxia. Consequently, the physiological effects of decreased hypoxic gene induction in $Arnt2^{-/-}$ neurons *in vivo* may be negligible, and they are clearly not sufficient to disrupt gross CNS development. Whole-mount PECAM immunohistochemistry on embryonic CNS revealed no obvious differences between wild-type and $Arnt2^{-/-}$ embryos, whereas $Arnt^{-/-}$ embryos had clear disruptions in the vascular endothelial network. This observation suggests that the expression of *Vegf* and other HIF-1 target genes in $Arnt2^{-/-}$ embryos is effectively normal, presumably because of the compensatory activity of ARNT. Given the observation that even modest decreases in VEGF expression can lead to profound angiogenic defects in other contexts (23, 24), the lack of morphological and vascular defects in the $Arnt2^{-/-}$ embryos supports this idea. In contrast, the vascular defects observed in the $Arnt^{-/-}$ embryos (Fig. 4*D*) were more severe than expected, as previous histological analysis (7) did not reveal the striking vascular anomalies reported for $Hif\text{-}1\alpha^{-/-}$ embryos (10, 11, 25). Finally, our results are in contrast to a previous report suggesting that ARNT2 is required for neuron survival (26).

In future work, it will be particularly interesting to determine whether loss of *Arnt2* function affects neural responses to ischemic insult. Several recent reports have implicated HIF complexes in modulating sensitivity to ischemic damage. RNAs encoding HIF-1α and several HIF-1 target genes are induced in tissues adjacent to ischemic infarcts in rats subjected to middle

cerebral artery occlusion (27). In addition, transient sublethal deprivation of oxygen and glucose leads to HIF stabilization in cultured cortical neurons, which correlates to enhanced resistance to subsequent lethal ischemic treatments (termed "preconditioning") (28, 29). The preconditioned state develops in a time-dependent fashion, suggesting that HIF-dependent expression of specific target genes may protect these neurons (29). A similar mechanism may explain the observation that increased expression of the GLUT1 glucose transporter, a known HIF-1 target, can protect vascular smooth muscle cells from hypoxia-induced apoptosis (30). Furthermore, HIF-1 has been implicated in stabilizing p53 in a variety of cell types (31, 32). Reduction of HIF-1α expression or mutation of p53 appears to regulate delayed neural death in murine cortical neuron cultures exposed to severe ischemic insult (33). The degree to which ARNT2 plays a role in preconditioning and p53-mediated neuronal death requires further investigation.

A strong genetic interaction between *Arnt* and *Arnt2* was revealed when compound heterozygous *Arnt*$^{+/-}$, *Arnt2*$^{+/-}$ mice were mated. Our results indicate that embryos with fewer than two wild-type alleles of either *Arnt* or *Arnt2*, in any combination, are absent or severely under-represented at E8.5. This finding suggests that either *Arnt* or *Arnt2* can fulfill one or more essential functions before E8.5, in a dose-dependent fashion, although *Arnt* subsequently becomes more critical to normal angiogenesis and development. The nature of these overlapping functions is unknown, but it is probable that only one wild-type allele of *Arnt* or *Arnt2* is insufficient to maintain the expression of essential shared target genes above a critical threshold before E8.5. Further work is required to determine the exact nature of the developmental arrest, but it is tempting to speculate that altered HIF function may be the cause of early lethality in the *Arnt*, *Arnt2* compound mutant mice. As embryos are faced with a hypoxic environment until approximately E8.5–E9.0 (5), and HIF complexes regulate the expression of glucose transporters and glycolytic enzymes (4), it is possible that compromised hypoxia-induced expression of these target genes could lead to general metabolic crisis. Interestingly, *Hif-1*$\alpha^{-/-}$ mutant embryos are indistinguishable from wild-type embryos at E8.5, indicating that other ARNT and ARNT2 partner proteins may also be involved (10, 11). In particular, HIF-2α and HIF-3α are attractive possibilities, as they have been shown to activate hypoxia-regulated genes in concert with ARNT (reviewed in ref. 4), although the activity of functionally distinct bHLH-PAS proteins cannot be excluded.

In summary, our analysis of the targeted *Arnt2*$^{-/-}$ mutation has revealed both unique ARNT2 functions (interaction with SIM1) as well as functions partly redundant with ARNT (hypoxic gene induction in cortical neurons, embryogenesis before E8.5).

We gratefully acknowledge J. Franklin Winslow, Fang Xong, and Min Min Lu for technical and histological assistance. Particular thanks are due to Michele Hadhazy for assistance with the blastocyst injections and mouse husbandry. We are also grateful for helpful discussions with Emin Maltepe, Andrew Arsham, and other members of the Simon laboratory. This work was supported by National Institutes of Health Grant HL62423 and the Howard Hughes Medical Institute.

1. Gu, Y. Z., Hogenesch, J. B. & Bradfield, C. A. (2000) *Annu. Rev. Pharmacol. Toxicol.* **40,** 519–561.
2. Reyes, H., Reisz-Porszasz, S. & Hankinson, O. (1992) *Science* **256,** 1193–1195.
3. Whitlock, J. P., Jr. (1999) *Annu. Rev. Pharmacol. Toxicol.* **39,** 103–125.
4. Semenza, G. L. (1999) *Annu. Rev. Cell Dev. Biol.* **15,** 551–578.
5. Maltepe, E. & Simon, M. C. (1998) *J. Mol. Med.* **76,** 391–401.
6. Chan, W. K., Yao, G., Gu, Y. Z. & Bradfield, C. A. (1999) *J. Biol. Chem.* **274,** 12115–12123.
7. Maltepe, E., Schmidt, J. V., Baunoch, D., Bradfield, C. A. & Simon, M. C. (1997) *Nature (London)* **386,** 403–407.
8. Kozak, K. R., Abbott, B. & Hankinson, O. (1997) *Dev. Biol.* **191,** 297–305.
9. Adelman, D. M., Maltepe, E. & Simon, M. C. (1999) *Genes Dev.* **13,** 2478–2483.
10. Iyer, N. V., Kotch, L. E., Agani, F., Leung, S. W., Laughner, E., Wenger, R. H., Gassmann, M., Gearhart, J. D., Lawler, A. M., Yu, A. Y. & Semenza, G. L. (1998) *Genes Dev.* **12,** 149–162.
11. Ryan, H. E., Lo, J. & Johnson, R. S. (1998) *EMBO J.* **17,** 3005–3015.
12. Maltepe, E., Keith, B., Arsham, A., Brorson, J. & Simon, M. (2000) *Biochem. Biophys. Res. Commun.* **273,** 231–238.
13. Hirose, K., Morita, M., Ema, M., Mimura, J., Hamada, H., Fujii, H., Saijo, Y., Gotoh, O., Sogawa, K. & Fujii-Kuriyama, Y. (1996) *Mol. Cell. Biol.* **16,** 1706–1713.
14. Michaud, J. L., Rosenquist, T., May, N. R. & Fan, C. M. (1998) *Genes Dev.* **12,** 3264–3275.
15. Wines, M. E., Tiffany, A. M. & Holdener, B. C. (1998) *Genomics* **51,** 223–232.
16. Michaud, J. L., DeRossi, C., May, N. R., Holdener, B. C. & Fan, C. (2000) *Mech. Dev.* **90,** 253–261.
17. Tybulewicz, V. L., Crawford, C. E., Jackson, P. K., Bronson, R. T. & Mulligan, R. C. (1991) *Cell* **65,** 1153–1163.
18. Jain, S., Maltepe, E., Lu, M. M., Simon, C. & Bradfield, C. A. (1998) *Mech. Dev.* **73,** 117–123.
19. Jing, X., Ratty, A. K. & Murphy, D. (1998) *Neurosci. Res.* **30,** 343–349.
20. Oike, Y., Takakura, N., Hata, A., Kaname, T., Akizuki, M., Yamaguchi, Y., Yasue, H., Araki, K., Yamamura, K. & Suda, T. (1999) *Blood* **93,** 2771–2779.
21. Schonemann, M. D., Ryan, A. K., McEvilly, R. J., O'Connell, S. M., Arias, C. A., Kalla, K. A., Li, P., Sawchenko, P. E. & Rosenfeld, M. G. (1995) *Genes Dev.* **9,** 3122–3135.
22. Crews, S. T. & Fan, C. (1999) *Curr. Opin. Genet. Dev.* **9,** 580–587.
23. Ferrara, N., Carver-Moore, K., Chen, H., Dowd, M., Lu, L., O'Shea, K. S., Powell-Braxton, L., Hillan, K. J. & Moore, M. W. (1996) *Nature* **380,** 439–442.
24. Carmeliet, P., Ferreira, V., Breir, G., Pollefeyt, S., Kieckens, L., Gertenstein, M., Fahrig, M., Vandenhoeck, A., Harpal., K., Eberhard, C., *et al*. (1996) *Nature (London)* **380,** 435–439.
25. Kotch, L. E., Iyer, N. V., Laughner, E. & Semenza, G. L. (1999) *Dev. Biol.* **209,** 254–267.
26. Drutel, G., Heron, A., Kathmann, M., Gros, C., Mace, S., Plotkine, M., Schartz, J. & Arrang, J. (1999) *Eur. J. Neurosci.* **11,** 1545–1553.
27. Bergeron, M., Yu, A. Y., Solway, K. E., Semenza, G. L. & Sharp, F. R. (1999) *Eur. J. Neurosci.* **11,** 4159–4170.
28. Bruer, U., Weih, M. K., Isaev, N. K., Meisel, A., Ruscher, K., Bergk, A., Trendelenburg, G., Wiegand, F., Victorov, I. V. & Dirnagl, U. (1997) *FEBS Lett.* **414,** 117–121.
29. Ruscher, K., Isaev, N., Trendelenburg, G., Weih, M., Iurato, L., Meisel, A. & Dirnagl, U. (1998) *Neurosci. Lett.* **254,** 117–120.
30. Lin, Z., Weinberg, J. M., Malhotra, R., Merritt, S. E., Holzman, L. B. & Brosius, F. C., 3rd (2000) *Am. J. Physiol.* **278,** E958–E966.
31. An, W. G., Kanekal, M., Simon, M. C., Maltepe, E., Blagosklonny, M. V. & Neckers, L. M. (1998) *Nature (London)* **392,** 405–408.
32. Ravi, R., Mookerjee, B., Bhujwalla, Z. M., Sutter, C. H., Artemov, D., Zeng, Q., Dillehay, L. E., Madan, A., Semenza, G. L. & Bedi, A. (2000) *Genes Dev.* **14,** 34–44.
33. Halterman, M., Miller, C. & Federoff, H. (1999) *J. Neurosci.* **19,** 6818–6824.